American Journal of Chemical Engineering
2020; 8(5): 112-124
http://www.sciencepublishinggroup.com/j/ajche
doi: 10.11648/j.ajche.20200805.12
ISSN: 2330-8605 (Print); ISSN: 2330-8613 (Online)

Simulating the Effects of Poisoning on the Rate of the Oxidation of Ammonia over a V_2O_5/TiO_2 Monolithic Diesel SCR Catalyst Using a Multichannel Model

Clas Ulf Ingemar Odenbrand

Department of Chemical Engineering, LTH Faculty of Engineering, Lund University, Lund, Sweden

Email address:
ingemar.odenbrand@chemeng.lth.se

To cite this article:
Clas Ulf Ingemar Odenbrand. Simulating the Effects of Poisoning on the Rate of the Oxidation of Ammonia over a V_2O_5/TiO_2 Monolithic Diesel SCR Catalyst Using a Multichannel Model. *American Journal of Chemical Engineering*. Vol. 8, No. 5, 2020, pp. 112-124.
doi: 10.11648/j.ajche.20200805.12

Received: September 2, 2020; **Accepted**: September 19, 2020; **Published**: October 30, 2020

Abstract: The background to this study is the need to find out if some reactions of O_2 oxidation of ammonia oxidation are important in the Selective Catalytic Reduction (SCR) of NO by NH_3. The objective of the study was to shed light on the influence of poisoning on these reactions over a diesel SCR catalyst by compounds in the exhaust gases. The method used was to experimentally determine the amounts of products formed at several temperatures and compared them to simulated values. About 700 ppm NH_3 was oxidized by 2% O_2 in helium yielding N_2, N_2O, and NO at increasing temperatures. Comparisons are given for a 4.56% vanadia on titania fresh catalyst and the ones used for 890 and 2299 h. The kinetics was simulated using a multichannel model of the monolithic catalyst. The experimental values of the products were nicely fitted by the kinetic model where all three ammonia oxidation reaction rates were of the first order in the concentration of ammonia. The fit was somewhat better for the non-isothermal case than the isothermal one. The deactivation reduces the activation energies for the formation of all products. Effects of flow and concentration maldistribution are shown to be present but are quite small. The temperature increase is 1.30 K for the most active catalyst at the highest temperature (733 K). The use of the multichannel model shows that quite considerable deviations in inlet ammonia concentrations are obtained over the catalyst cross section. This means that the catalyst is not used to its full potential.

Keywords: Oxidation of Ammonia, Poisoning and Kinetics, Monolithic Multichannel Model, Vanadia SCR Catalyst

1. Introduction

The Selective Catalytic Reduction (SCR) technique is today a required method for removing NO_x from mobile applications in many countries. Marine engines run under conditions, which resemble the ones in stationary diesel power plants. In 2017, there were hundreds of SCR units installed on diesel engines on ships [1]. The lubricating oil for the diesel engine is often a source for deactivation components for the catalyst. The Ca, Zn, P, and S will deactivate the SCR catalyst, as shown in previous publications [2, 3]. In those studies, it was shown how the activity and selectivity in the SCR reaction system are influenced by poisoning.

In 1993 Ozkan et al. [4] studied the role of ammonia oxidation in the SCR over vanadia catalysts. They found that N_2, N_2O, and NO were the products. In their extensive study [5] using nitrogen labelling, they discovered that the ammonia species giving N_2 and N_2O have relative long residence times on the surface. The NO producing species are short-lived though. Thus, three ammonia oxidation reactions are assumed. Duffy et al. [6], using V_2O_5/TiO_2 catalysts with varying vanadia contents, also used isotopic labelling studies to conclude that below 300°C $^{14}N^{15}N$ is always the first product from ^{15}NO and $^{14}NH_3$. At higher temperatures, the product distribution is susceptible to the vanadia content of the catalyst. At 500°C, 70% of the product is ^{14}NO. Pure V_2O_5 produces significantly more $^{14}N^{15}NO$, and at lower temperatures than a 1.4 wt% V_2O_5/TiO_2 catalyst. As part of an SCR study, the kinetics of the partial ammonia oxidation giving N_2 was studied between 250 and 300°C by Efstathiou et al. [7]. They studied the oxidation of 1000 ppm NH_3 by 2% O_2 with helium as background gas over an 8 mol% V_2O_5/TiO_2 catalyst. The

selectivity to N_2 was from 98.2 to 97.6% decreasing with temperature. The rate of the ammonia oxidation was only from 1.8 to 2.4% of the SCR reaction rate. Djerad et al. [8] included all three NH_3 oxidation reactions in their study on the effect of oxygen on the reaction rates. Using a 3%V, 9% W on titania catalysts, the impact of oxygen was small between 2 and 15% O_2. A maximum in the formation of N_2 was observed at 425°C, N_2O was formed above 300°C but NO only above 425°C. They found that the creation of N_2O from ammonia oxidation is essential in the SCR process.

In the study by Usberti et al. [9], low concentrations, 33, 150, and 333 ppm, of ammonia was oxidized by 3.5% O_2 in the presence of 2% H_2O. The background gas was nitrogen, so this product could not be detected. They explain their results by oxidation reactions leading to NO, which reacts further with NH_3 by the normal SCR reaction. Their findings contradict the ones in this study which explain the results by only ammonia oxidation reactions.

Chae et al. [10] modelled and simulated the SCR process using experimental data from a catalytic bed. They developed models for extruded as well as wash coated monoliths. They showed that even with a catalyst layer thickness of 54 m, the effectiveness factor was only 0.6 for the SCR reaction, indicating diffusion resistance in a V_2O_5-WO_3/TiO_2 catalyst. The ammonia oxidation to NO was used in their study. Nova et al. [11] studied the thermal deactivation of commercial V_2O_5-WO_3/TiO_2 deNO_X catalysts. In the direct oxidation of NH_3 using the Temperature Programmed Reaction (TPR) experiments with 840 ppm NH_3 and 2% O_2 in helium, they observed N_2 from 327°C and N_2O from 427°C. Both compounds increase continuously with temperature up to 500°C. No nitric oxide (NO) was formed on the catalyst calcined at 500°C. When calcined at 800°C, NO was created in addition to N_2 and N_2O. No kinetic expressions were given though.

Chen et al. [12] performed a simulation study on a catalyst bed using the commercial program COMSOL Multiphysics. They optimized the performance of the reactor using only the SCR and the direct oxidation of NH_3 to N_2 (SCO) reactions. Yun and Kim [13] modelled SCR over vanadia-based catalysts from heavy-duty diesel exhaust gases. The chemical reactions they used were the SCR, the fast SCR where NO plus NO_2 react with NH_3 to N_2, and the oxidation of NH_3 to NO. They used the assumption that simulation of one channel would represent the performance of the whole monolith. Using the SCR and the SCO, Om et al. [14] modelled a monolith reactor for the SCR process. In 2017 Millo et al. [15] simulated the SCR system using a 1-D fluid-dynamic simulation code with the SCR and the SCO reactions. Åberg et al. [16] performed a detailed study using MATLAB comparing a reference model, including all critical parameters, to simplified models. The reactions were the NH_3 oxidation to NO, the SCR, and the fast SCR. The model was able to predict the catalyst output during the European Transient Cycle (ECT cycle). A recent paper [17] presented a method to simulate the kinetics of the SCR reactions as well as many of the NH_3 oxidation ones to obtain novel and better monolith channel designs. The results are detailed showing, among others, the temperature profile in the catalyst bed when converting 1500 ppm NO with NH_3 in the SCR process. They also consider the shape of the monolith channel showing that the most effective one is a hexagonal one.

In a recent paper [3], results are presented from the oxidation of ammonia over fresh and deactivated vanadia on titania catalysts using simulation with a single-channel model. The results were presented mostly as isothermal cases. It is therefore of interest to study a multichannel model under non-isothermal conditions. The multichannel model presented in this paper shows the details of how the flow distribution affects the activity and selectivity in the ammonia oxidation. Effects of maldistribution, on the reactor performance, of temperature, and component concentrations will also be shown.

The deactivation procedure used decreased the surface area sharply after 890 h. Only a small further reduction in area is obtained at 2299 h of deactivation. The catalyst used is a thin layer vanadia supported on cordierite where the effects of deactivation will be visible because of the small amount of catalyst present. At the same time, the 20 m thick catalyst layer is thin enough for internal diffusion effects to be minimal.

The data used in the present study were measured at two increasing degrees of poisoning by the compounds most likely to be present on catalyst after commercial use. Therefore, the result could be used in the design of new catalysts for diesel engines which are deactivated by compounds in the lubrication oil.

2. Experimental

2.1. Preparation and Deactivation of the Catalyst Samples

The catalysts used were made in house by a Swedish catalyst manufacturer and consisted of 5.64% V_2O_5 on TiO_2 (Rhone Poulenc DT (8)) on the support of cordierite from Corning with 400 Cells Per Square Inch (CPSI). Details on the preparation, deactivation and characterization can be found in Odenbrand [3]. The accelerated test was supposed to simulate the regular running of a truck for up to 500 000 km (given by the catalyst manufacturer).

2.2. Measurements of Catalyst Activity and Selectivity

Activities and selectivities were measured on 1 cm mini monoliths as described before [17] by mass spectrometry using helium as a background gas. The piece five from the inlet was used in the ammonia oxidation experiments. This piece was chosen because of its low but still noticeable degree of poisoning. The activity and selectivity in the oxidation of ammonia with O_2 were measured at about 700 ppm NH_3 and 2% O_2. The pressure was 1.24 bar (Space velocity 45 000 h^{-1}). Temperatures were from 380 to 460°C (653 to 733 K) at 20°C intervals. Helium was used as a background gas containing about 3000 ppm of Ar for internal calibration. The background concentrations of N_2 and H_2O were 37.7 ± 0.2 and 31.4 ± 2.5 ppm respectively showing the accuracy of the mass spectrometric data. The inlet concentrations of NH_3 were 729, 746, and 702 ppm for the fresh

catalyst, the ones used for 890 h, and 2299 h. For N_2O, the following inlet concentrations were measured 1.2, 1.0, and 2.0 ppm, respectively. Also, for NO, they were 4.6, 3.8, and 4.0 ppm. The actual levels were used in the simulation of each series of experiments.

2.3. The Multichannel Model of the Catalyst Monolith

The full monolith contains 81 channels. The multichannel model uses the geometry shown in Figures 1 and 2. In the simulations, one-eighth of the entire reactor is used. The experimental setup includes an inlet tube with 2 mm inside diameter which feeds the gas to the reactor and is included in the multichannel model. High inlet velocities in the center of the reactor could cause problems with maldistribution of reactants at the inlet of the monolith. This phenomenon can quickly be addressed using the simulation program.

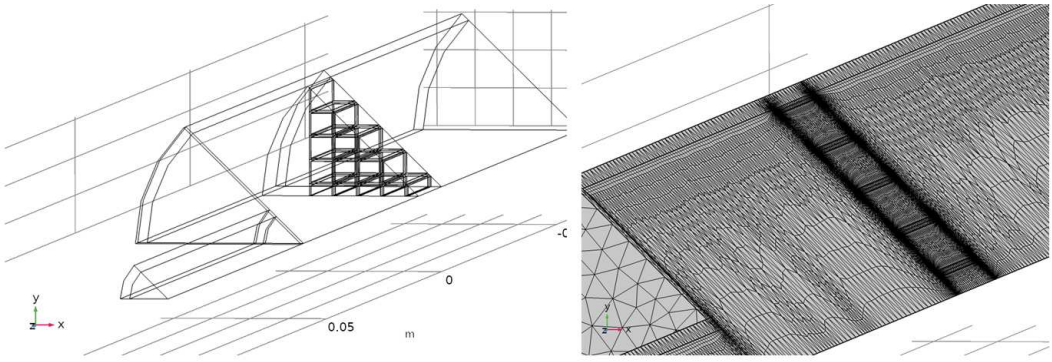

Figure 1. *Left, 1/8 of the whole monolith showing the 2 mm inner diameter inlet tube without meshes for clarity. The square mini monolith consists of non-porous cordierite, is 1 cm long and has a catalyst layer on all walls. The right part of the figure shows the mesh size "normal" (772,241 total number of elements). Boundary layers are present both in the open channel and along with the catalyst layer.*

Figure 2 shows the details of the catalyst part of the reactor with the quartz glass wall, the quartz wool stopping, and the cordierite monolith with a 21 μm catalyst layer supported on it.

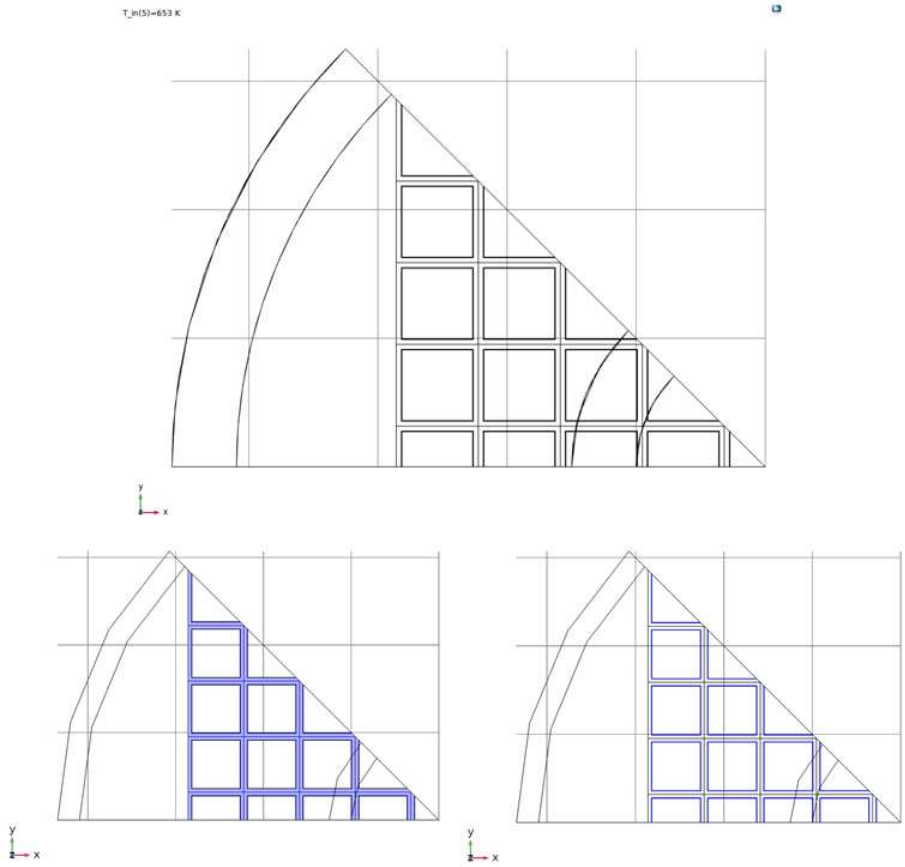

Figure 2. *The detail of the part of the monolith studied in the multichannel model. Top row to the left, the quartz glass tube, the quartz wool filling and the cordierite monolith. Top row to the right, the cordierite catalyst support. Bottom row to the left, the 21 μm catalyst layer inside all channels of the monolith.*

2.4. Stationary Modelling of the Catalytic Reactor

COMSOL Multiphysics ver. 5.5 was used in the simulations in a similar way as described before [18, 19] but with a different monolithic model with physical data given in Table 1. The processor was an Intel i7 9700K octa-core operating at 3.6 GHz using a maximum of 64 GB of a 2666 MHz memory. The physic-controlled mesh was used with the "coarser" element size (The total number of elements is 241,914) for preliminary studies. When a physics-controlled mesh is used, three boundary layers close to the walls are introduced by the program to get a fine resolution of the velocity profile in those positions. The simulations were performed for non-isothermal cases. The heat was conducted to the reactors outside, according to Q_0=h*(Tin-T). The heat transfer constant (h) was taken as 100 W/m^2/K [18]. The solution for all cases was obtained by performing two separate stationary studies. The process was simulated in a stationary mode in 2 studies. In the stationary study, one, used to get starting values for study two, the calculations were performed in 3 steps. The Free and Porous Media Flow node was calculated in step 1 at 733 K. In step 2 (733 K), the following nodes were used, Free and Porous Media Flow, Chemistry, and Transport of Diluted Species. Finally, in step 3 (733 K), all above nodes were used in addition to Heat Transfer in Porous Media. In the stationary study two, all nodes were used, and initial values of variables were taken from study one step three. The temperature was decreased from 733 downwards to 613 or 653 K in stages of 20 K using an auxiliary step procedure. The stationary solver used was PARDISO with a relative tolerance of 0.001. The variables u and p were solved in segregated step one, all concentrations in step two, and the temperature in step three.

The fitting procedure is such that first, a mesh size "coarse" (The total number of elements is 425,512) is used. Nitrogen is first fitted. Then simultaneously N_2O and NO. The mesh size was refined until the constant values of the outlet concentrations were obtained. Finally, the mesh size is changed to "normal" (The total number of elements is 772,241), and the improvement in results is studied. The process is guided by the relative total sum of squares of errors (see below) which is minimized. Manual changes in kinetic parameters are performed to fit the simulated values to the experimental ones according to the method described before [18, 19].

2.5. Solution in COMSOL Multiphysics

2.5.1. Chemistry

$$R_i=\Sigma_j R_{ij}$$

This part of the program is used to define and calculate the chemical rates. The R_{ij} are given as Arrhenius expressions in Table 2. In all cases, the e ect of oxygen, present in excess (2%), is included in the rate constant. In this part, data are supplied to calculate transport and thermodynamic data as a function of the temperature. Helium is used as a solvent.

Table 1. *Physical data used in the Transport of Diluted Species, the Free and Porous Media Flow, Heat Transfer in Porous Media nodes in the COMSOL program.*

Parameter	Open channel Mainly helium	Catalyst Layer Vanadia/Titania	Catalyst support Cordierite
Diffusion coefficients for NO in fluid *10^4 (D_{fluid}, m^2/s)	2.27 - 2.75	n.a.	n.a.
Diffusion coefficients in catalyst (m^2/s)	n.a.	$D_{eff}=\varepsilon/\tau*D_{fluid}$ $\tau=\varepsilon-(1/3)$	n.a.
Porosity of titania catalyst (ε)	n.a.	0.4	n.a.
Density at inlet conditions (kg/m^3)	0.080 – 0.080	2,295	2,600
Dynamic viscosity *10^5 (Pas)	3.412 – 3.678	n.a.	n.a.
Permeability (m^2)	n.a.	$6*10^{-8}$	n.a.
Thermal conductivity (W/(m*K))	0.266 – 0.287	0.2	3
Heat capacity (J/(kg*K))	5,200	690	1,463

n.a. Not applicable.
The ratio of specific heats is 1 in all domains.
Values are given at 653 and 733 K.

Table 2. *The base case for the chemical reactions and the kinetic expressions used in the simulations.*

Reaction number	Global reaction	Rate expression	The heat of reaction (kJ/mol)
1	$4NH_3+4NO+O_2=>4N_2+6H_2O$	$r_1=A_1*\exp(-E_1/(R*T))*c_{NO}*\theta_{NH3}$	Not used
2	$4NH_3+3O_2=>2N_2+6H_2O$	$r_2=A_2*\exp(-E_2/(R*T))*c_{NH3}$	1263
3	$4NH_3+4NO+3O_2=>4N_2O+6H_2O$	$r_3=A_3*\exp(-E_3/(R*T))*c_{NO}*\theta_{NH3}$	Not used
4	$4NH_3+4O_2=>2N_2O+6H_2O$	$r_4=A_4*\exp(-E_4/(R*T))*c_{NH3}$	1133
5	$4NH_3+5O_2=>4NO+6H_2O$	$r_5=A_5*\exp(-E_5/(R*T))*c_{NH3}$	897

The reactions are demanding more and more oxygen and are being more important at increased temperatures; the higher the number of the reaction is (Table 2). It is only reactions 2, 4 and 5 that have a significant influence on the kinetics of ammonia oxidation because of deficient concentrations of NO in the system. Thus, reactions 1 and 3 are omitted in this study.

2.5.2. Transport of Diluted Species

This part of the program is used to calculate the concentrations of all components (NH_3, N_2, N_2O, NO, H2O, O_2, and He). The slip through the walls is 0. The inlet

concentrations of all species are known and given in section 2.2 above.

$$\nabla*J_i+u*\nabla c_i=R_i$$

$$J_i=-D_i\nabla c_i$$

c_i is the concentration of the species (mol/m^3)
D_i denotes the diffusion coefficient (m^2/s)
R_i is the reaction rate expression for the species (mol/(m^{3}s))
u is the mass averaged velocity vector (m/s)
J_i is the mass flux diffusive flux vector (mol/(m^{2}s))

2.5.3. Free and Porous Media Flow

This part is used to calculate the velocity and the pressure from the inlet and the outlet conditions. The inlet condition is u=vin perpendicular to the inlet surface. The outlet condition is $p=p_{tot}-p_{ref}$. The reference pressure is the atmospheric pressure. The Chemistry node calculates density and dynamic viscosity.

$$\rho(u*\nabla)u=\nabla*[-p*I]$$

$$\rho\nabla*u=0$$

ρis the density (kg/m^3)
p is the pressure (Pa)
I is the moment of inertia (kgm^2)

2.5.4. Heat Transfer in Porous Media

This part is used in the non-isothermal cases and calculates the temperature in the system. Heat, evolved by the chemical reactions in the catalyst, and transported through the system causes the temperature to increase. Q (q in the equation above) is the heat that flows from the reactor to its outside.

$$\rho C_p u*\nabla T+\nabla*q=0$$

$$q=-k_{eff}\nabla T$$

C_p is the specific heat capacity at constant pressure (J/kgK)
T is the absolute temperature (K)
k_{eff} is the effective thermal conductivity (W/mK)
q is the heat transferred (J/m^{2}s)

2.6. General Simulation Conditions

The physical properties used in the simulations are given in Table 1. Incompressible flow with a normal inlet velocity of vin in the direction of the reactor axis was used for the Free and Porous Media Flow node. The total flow (Q_{in}) at NTP was 0.9 l/min was introduced into the large tube containing the catalyst block trough a stainless-steel tube with an inner diameter of 4 mm in the multichannel model. The circular inlet area of the tube (A_{in}) was 1.265*10^{-5} m^2. The reference pressure (p_{ref}) was 1 bar, and the total one (p_{tot}) at the reactor exit was 1.236 bar. Thus, $v_{in}=Q_{in}/A_{in}*Tin/273.15/p_{tot}*p_{ref}$ (2.593 m/s at 733 K (460°C)). The program calculates the varying inlet velocities at different inlet temperatures (T_{in}).

The thickness of the catalyst layer was to 21 μm as described before [3]. The catalyst layer was supposed to cover all inside walls of the monolith. The reactor, made of quartz glass, is 100 mm long with the bottom of the catalyst monolith (1 cm long) positioned 60 mm from the inlet on a plug of glass wool. The monolith was surrounded by quartz wool to stop gas bypassing the catalyst. Only a small part of the simulated system is shown to detail the size of the mesh used in the calculations.

2.7. Criteria for Evaluation of the Best Fit

When comparing simulations, it is necessary to use the relative sum of squares of errors (SSE_{reltot}) of the whole data set. Each set of experimental concentration data is first divided by its maximal value (at T=733 K) yielding

$N_2rel=N_2(Tin)/N_2exp(733)$
$N_2Orel=N_2O(Tin)/N_2Oexp(733)$
NOrel=NO(Tin)/NOexp(733)

Then, the simulated values are divided by the same maximum value yielding simulated relative values for each component.

$N_2relsim=N_2sim(Tin)/N_2exp(733)$
$N_2Orelsim=N_2Osim(Tin)/N_2Oexp(733)$
NOrelsim=NOsim(Tin)/NOexp(733)

The SSE for each component is calculated as

$SqN_2=(N_2rel-N_2relsim)^2$
$SqN_2O=(N_2Orel-N_2Orelsim)^2$
$SqNO=(NOrel-NOrelsim)^2$

Finally, the individual values are added up for all temperatures to SSEreltot.

$SSE_{reltot}=SqN_2 + SqN_2O + SqNO$
n=number of experimental points
Mean deviation=$(SSE_{reltot}/n)^{0.5}$

3. Results and Discussion

3.1. Catalyst Characteristics

The deactivated catalysts have been analyzed for their surface compositions of Ca, P, Zn, and S [2] usually compounds present in the fuel and especially lubrication oil.

Table 3. *Some characteristics of the catalysts studied.*

Time of use (h)	Ca/Ti	P/Ti	Zn/Ti	S/Ti	S_{BET} (m^2/g)	Pore vol. (cm^3/g) *10^3
0	n.a.	n.a.	n.a.	n.a.	12.7	5.5
890	0.111	0.642	0.102	0.083	7.8	4.9
2299	0.361	0.164	0.026	0.027	7.1	4.0

n.a. not analyzed. The Ca/Ti and other contents were measured by XPS [2].

From the results shown in Table 3 one can assume that Ca is present at the very uttermost layers of the catalyst surface since its content increases with time of use. Part of the S also stays at the surface probably as $CaSO_4$. $CaSO_4$ has been shown before to deactivate similar catalysts [19]. P, Zn, and S do also penetrate the catalyst layer and therefore their contents on the surface are lower at the longest times. The contents of P and Zn on the surface after 2299 h are about 25% of that after 890 h. Even so, the experimental rates for most of the reactions are lowest on the catalyst used for 2299 h. Thus, one must assume that these compounds penetrate deeper into the catalyst layer causing the lower activity.

There is a strong influence of the deactivation procedure on the surface area and the pore volume (Table 3). The catalyst used for 890 h has only 61% of its original surface area left.

After 2299 h the surface area decreases to 55% of its original value. The pore volume is not so drastically reduced, but by13% after 890 h and by 27% after 2299 h. Thus, the surface area seems to stabilize after some time while the pore volume continues to decrease on deactivation almost proportionally to the time of use. Earlier studies show that the smallest pores are eliminated by sintering or pore filling with poisons [2].

3.2. Fit of the Simulated and Experimental Concentrations

As Figure 3 shows is it possible to nicely fit the experimental concentrations of N_2, N_2O and NO, as direct reaction products of the oxidation of ammonia, to the ones simulated by the model.

Figure 3 top left shows the concentration of N_2 in the reactor exit and its variation with the temperature for the fresh catalyst. It varies from 85 to 156 ppm for the fresh catalyst, from 89 to 155 ppm for the catalyst used for 890 h, and from 45 to 80 ppm for the catalyst used for 2299 h. Considering that two ammonia are needed to produce one N_2 the conversions are 13.2 to 32.8%, 13.9 to 31.6%, and 12.8 to 33.3% for the three catalysts. Thus, there is not a large difference in the conversions of NH_3 to N_2 among the catalysts.

The products N2O and NO are present as 32 and 13 ppm, 54 and 24 ppm, and 44 and 38 ppm for the three catalysts at the highest temperature. Corresponding conversions of NH_3 to the products are 8.3, 14.2, and 12.0 for N_2O and 1.16, 2.71, and 4.84 for NO, for the three catalysts, respectively.

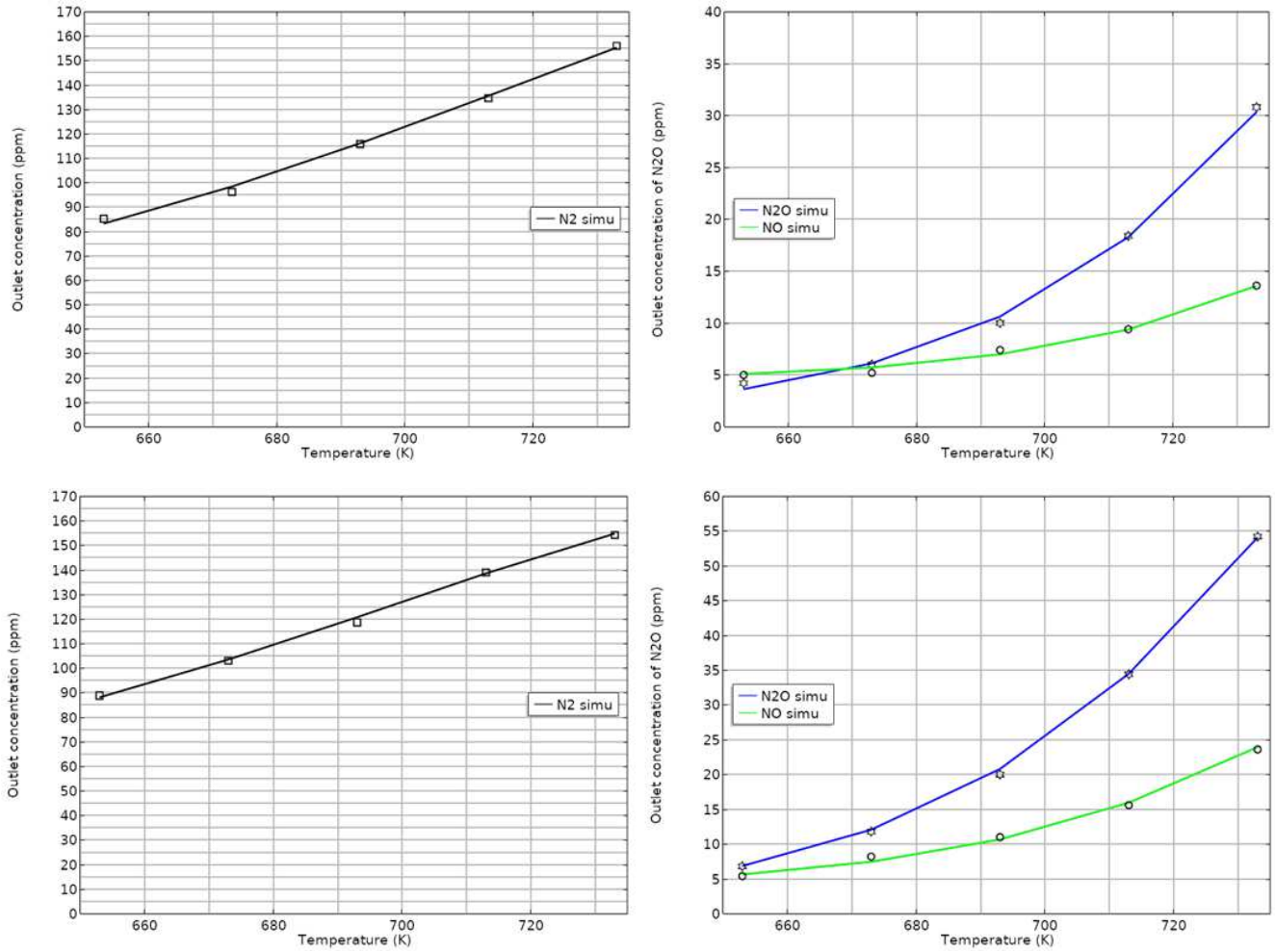

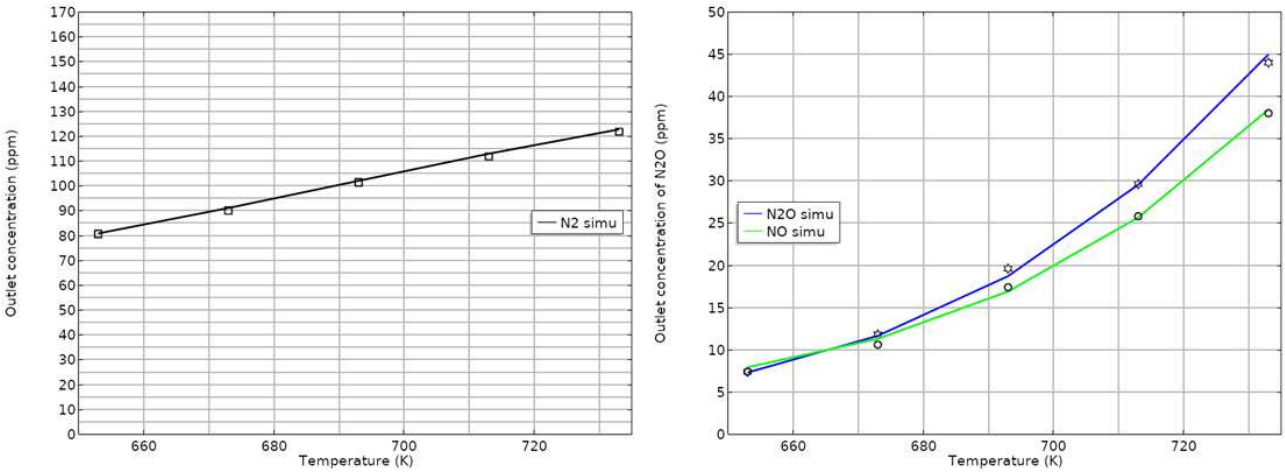

Figure 3. *The effect of the deactivation on the fit of concentrations of N_2, N_2O, and NO. Oxidation of about 700 ppm NH_3 with 2% O_2 in helium for catalysts used for different amounts of time. Top row fresh catalyst, middle row catalyst used for 890 h, and bottom row catalyst used for 2299 h.*

3.3. Kinetic Parameters

Table 4. *Kinetic parameters in the oxidation of about 700 ppm NH_3 with 2% O_2 in Helium. Rates are given at 653 and 733 K and inlet concentrations.*

Parameter/Catalyst	Fresh isotherm	Fresh non-isotherm	890 h isotherm	890 h non-isotherm	2299 h isotherm	2299 h non-isotherm
A_2*10^{-6} (s^{-1})	3.39	3.10	2.15	2.23	0.26	0.25
E_2 (kJ/mol)	64.5	64	61.5	61.75	50.75	50.5
R_2 (mol/m^3s)	0.389-1.220	0.392-1.228	0.439-1.293	0.435-1.297	0.366-0.868	0.366-0.868
A_4*10^{-11} (s^{-1})	2.39	2.14	1.22	0.62	0.16	0.12
E_4 (kJ/mol)	141	140.5	133	129	122	120.5
R_4 (mol/m^3s)	0.0209-0.307	0.0206-0.303	0.0475-0.588	0.0505-0.584	0.0442-0.443	0.0450-0.434
A_5*10^{-11} (s^{-1})	9.49	9.47	0.994	0.532	0.234	0.094
E_5 (kJ/mol)	161	161	142	138.25	130	124.5
R_5*10^3 (mol/m^3s)	2.08-45.7	2.09-46.4	7.36-109	7.93-112	14.9-175	16.6-173
$SSE_{reltot}*10^3$	4.8508	4.464	3.1504	3.6098	2.7866	2.1471
Dev. (%)	1.80	1.73	1.45	1.55	1.36	1.20
Time (s)	3544	3928	3467	4618	3271	3637
dT (K)	n.a.	1.08	n.a.	1.30	n.a.	0.95

dT is presented at 733 K, n.a. not applicable. Dev.=Deviation.

Table 4 shows that the activation energy decreases when the catalyst gets more deactivated, as explained before [20, 21]. All three reactions behave similarly in this respect. The poisoning has the most substantial effect on the formation of NO with an increased amount of NO on the poisoned catalyst.

Kinetic parameters do not change very much when non-isothermal conditions are introduced using the "normal" mesh size. When the "fine" mesh size is used, exceptionally long simulation times are needed and large amounts of memory, slowing down the process too much for only a small change in parameters obtained (not shown here).

We compare our values to Chen and Tan [12] who also used COMSOL Multiphysics in the simulation of, in their case, a V_2O_5 on TiO_2 catalyst bed. Their value of E_2 is 84.4 kJ/mol for the formation of N_2 (R_2) when corrected for diffusion limitations while our apparent value is 64 kJ/mol for the fresh catalyst. The values of k_2 ($A_2*\exp(-E_2/(R*T))$ were $6.73*10^7$ and $3.10*10^6$ s^{-1}, respectively. The rate constant at 653 K is thus 11.9 for Chen and 23.5 s^{-1} in this study. Remarkably similar values. Are the rates of formation of N_2 large enough to be influenced by washcoat diffusion? The thickness of the catalytic layer is 21 μm, and the Thiele modulus is 0.0293 leading to an effectiveness factor of 0.99975 at 460°C. Thus, all lower temperatures will be diffusion free too. The high value of the effectiveness factor in our study can be compared to the data of Chae et al. [10] where they state that for a wash coated 2 wt% V and 6 wt% W, V_2O_5-WO_3/TiO_2 catalyst with a 54 μm catalyst layer the effectiveness factor in the SCR reaction was 0.6 at 300°C and 0.2 at 460°C. The rates of the oxidation of ammonia are lower than the rates of the SCR reaction and can explain the difference.

Efstathiou and Fliatoura [7] determined the apparent activation energy of 61.4 kJ/mol for the oxidation of 1000 ppm NH_3 with 2% O_2 in helium for an 8 mol% (16.5 wt%) V_2O_5/TiO_2 catalyst from experimental rates. The rate of N_2 formation at 300°C was $17.2*10^{-6}$ mol/g/min compared to ours calculated one of $7.62*10^{-2}$ $mol/(m^3s)$ ($1.99*10^{-6}$ mol/g/min) for the fresh catalyst. Thus, rates are in the same range. The difference can be explained by that their catalyst contained more V_2O_5 than ours.

The formation rates of N_2 (R_2), as shown in Table 4, are

about the same for the fresh catalyst and the one used 890 h. The catalyst used for 2299 h, has a lower rate of formation of nitrogen at all temperatures. The rates of formation of N_2O (R_4) are about 0.2, 0.57, and 0.44 mol/m^3/s for catalysts used for 0, 890, and 2299 h. On the other hand, the rate of formation of NO (R_5) increases as 0.046, 0.108, and 0.173 mol/m^3/s with an increased degree of poisoning at 460°C. If we assume that, the rate of reaction 2 is the same under SCR conditions as under NH_3 oxidation conditions, we can compare the values of Salehi et al. [22] to ours, since they also used first-order dependence on NH_3 concentration. They also simulated a monolithic structure with a catalyst layer. Their values of k_2 and E_2 were 6.8*10^7 and 85 compared to ours of 3.1*10^6 s^{-1} and 64 kJ/mol, respectively. We calculate the rate R_2 at 653 K from Salehi's [22] data to 0.159 compared to ours of 0.347 mol/m^3/s. They are in the same range.

Om et al. [14] studied, using Fluent, the SCR in a monolith isothermally. The concentrations of NO and NH_3 were in the range of 1000 ppm, so we believe that the simulation should have been non-isothermal for more precise results. Their data were based on an experimental study on a catalytic filter by Schaub et al. [23], so the values of the rate parameters should be close to intrinsic values, and k_2 and E_2 were 6.73*10^7 and 85.4 kJ/mol. At the same time, ours were 3.1*10^6 and 64 kJ/mol, respectively (Table 4). Calculation of nitrogen formation rates at 653 K from their data gave a value of 0.183 while our value was 0.19 mol/m^3/s. The rates are remarkably close. At 460°C their rate was 0.91 and ours 1.24 mol/m^3/s.

Millo et al. [15] simulated the SCR on a filter catalyst for automotive applications. Besides the standard SCR, the fast and slow SCRs, the oxidation of NH_3 to N_2 was used as model reactions. The activation energy (E_2) was 144.6 kJ/mol, much higher than our value of 64 kJ/mol. Their rate expression was $r_2=k_2'*c_{NH3}*c_{O2}$ includes the dependence on the oxygen concentration making direct comparisons hard. Their experiments also included water which would decrease the rate of all reactions.

There is a maximal rate for all oxidation rates but the oxidation to NO for the catalyst used for 890 h. Formation of new acidic sites, from sulphur species, is a probable cause for this maximum. The uncorrected, non-isothermal, rate of formation of N_2 (R_2) increases from 1.228 via 1.297 and decreases to 0.868 mol/m^3/s from 0 via 890 to 2299 h of use. The first increase is 5.6%. The decrease at 2299 h is 29.3% from the fresh one.

3.4. Surface Specific Rates

The rates given in Table 4 are recalculated as surface specific rates since the BET surface area shrinks considerably during the deactivation process as described above.

Table 5. *Surface specific rates for the oxidation of 700 ppm NH_3 with 2% O_2 in Helium. Rates are given at 653 and 733 K and inlet concentrations.*

Surface specific rate (mol/m^{3}s /m^2/g)	Catalyst					
	Fresh iso	Fresh non-iso	890 h iso	890 h non-iso	2299 h iso	2299 h non-iso
R_2/S_{BET} *10^3	30.5-95.8	30.8-96.4	56.5-166	56.0-167	51.8-122.9	51.8-122.9
R_4/S_{BET} *10^3	16.4-24.1	16.2-23.8	61.1-75.7	65.0-75.2	62.6-62.7	63.7-61.5
R_5/S_{BET} *10^4	1.63-35.9	1.64-36.4	9.47-140	10.2-144	21.1-248	23.5-245

iso=isothermal, non-iso=non-isothermal.

When the non-isothermal surface-specific rates are compared at 733 K (Table 5), they are 96.4, 167, and 122.9 *10^{-3} mol/m^3/s/m^2/g, for the three catalysts. Thus, a 73% increase is observed at 890 h from the fresh catalyst. At 2299 h of use the increase is 27% compared to the fresh one. Thus, both deactivated catalysts are more active than the fresh one per surface area unit. At 653 K the non-isothermal surface-specific rates are 30.8, 56.0, and 51.8 *10^{-3} mol/m^3/s/m^2/g, respectively.

The non-isothermal surface-specific rates for the formation of N_2O at 773 K are 23.8, 75.2, and 61.5*10^{-3} mol/m^3/s/m^2/g, respectively for the three catalysts. Both these reactions have maximum activities at 890 h of use.

The rate of formation of NO behaves differently being 36.4, 144, and 245*10^{-4} mol/m^3/s/m^2/g at 733 K. Thus, the rate of formation of NO increases continuously with the degree of poisoning. Such a result is in line with them by Due-Hansen et al. [24] who studied the K poisoning of V_2O_5-WO_3/ZrO_2 catalyst in ammonia oxidation. An increased poisoning caused an increased formation of NO.

3.5. Temperature Increase Caused by the Reactions

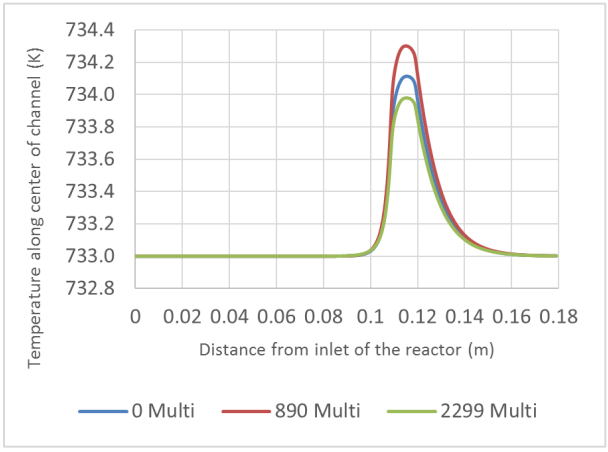

Figure 4. *The simulated temperature along the center of the reactor for the three catalysts studied. Inlet temperature 733 K.*

Table 4 shows that the maximal rate is obtained for the catalyst used for 890 h. This results in the highest temperature increase for this case (Figure 4, red curve, 1.3 K, inlet temperature 733 K). The catalyst inlet is situated 11 cm from

the reactor´s inlet. The temperature starts to increase before it reaches the monolith and is 734.1 K at its inlet for the catalyst used for 890 h. It increases to a maximum of 734.3 K inside the monolith. The maximal temperature for the fresh catalyst and for the one used for 2299 h are734.1, and 734.0, respectively. Thus, the temperature increases correlated fine with the rates in Table 4.

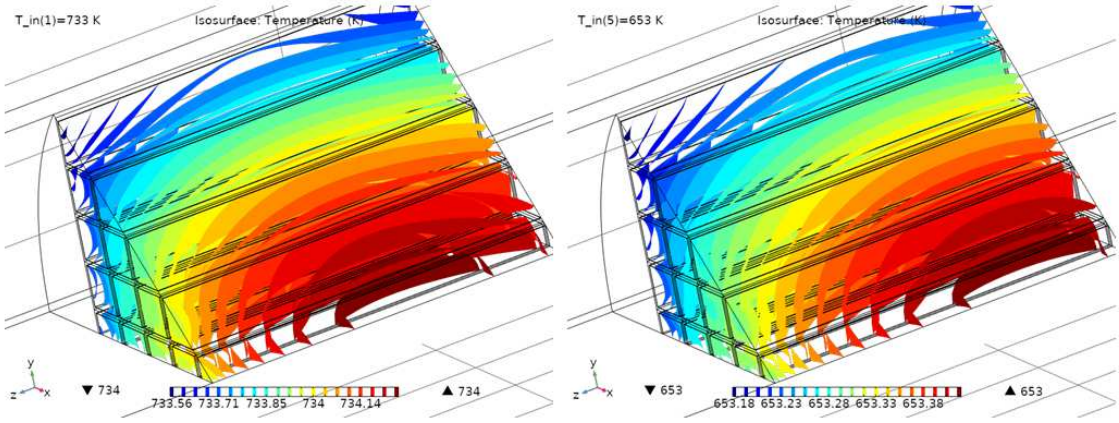

Figure 5. *Temperature distribution in the monolith section of the catalyst used for 890 h. Left, at 733 K, and right, at 653 K.*

Figure 5 shows that at 733 K inlet temperature, the maximal temperature increase (1.30 K) is in the center of the catalyst block and is located at around 4 mm from the exit of the monolith. At 653 K inlet temperature, the increase (0.43 K) is at 2 mm from the outlet of the monolith. The higher the temperature, the closer to the catalyst inlet is the maximal temperature which is expected. A maximal temperature in the center of the catalyst block is expected since the heat of reaction is transported towards the outer side of the block. The temperature outside of the reactor is equal to T_{in} and is cooling the catalyst.

3.6. Velocity Distribution

Figure 6 shows how the velocity magnitude decreases sharply from 5.25 m/s in the center of the inlet tube to almost 0 close to the walls in the large quartz tube. There remains a maldistribution in flow in the middle of the channel with a speed of 0.26 m/s just before the catalyst section. Inside the small channels of the monolith the maximal rate is about 0.79 m/s in the center of most channels.

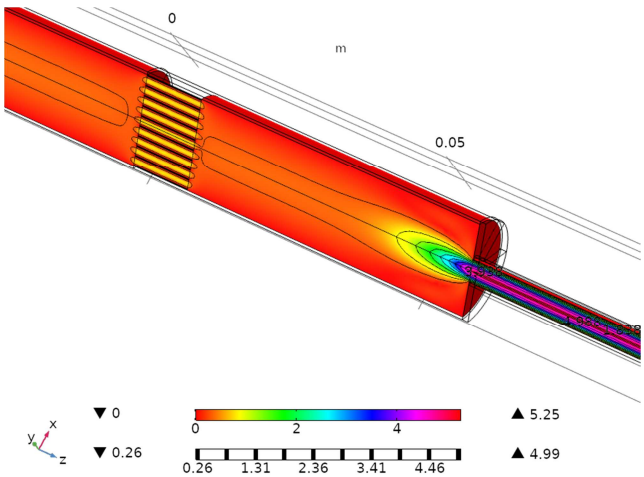

Figure 6. *The velocity magnitude (m/s) along the catalyst system. The catalyst used for 890 h at an inlet temperature of 733 K, and an NH_3 inlet concentration of 745.6 ppm.*

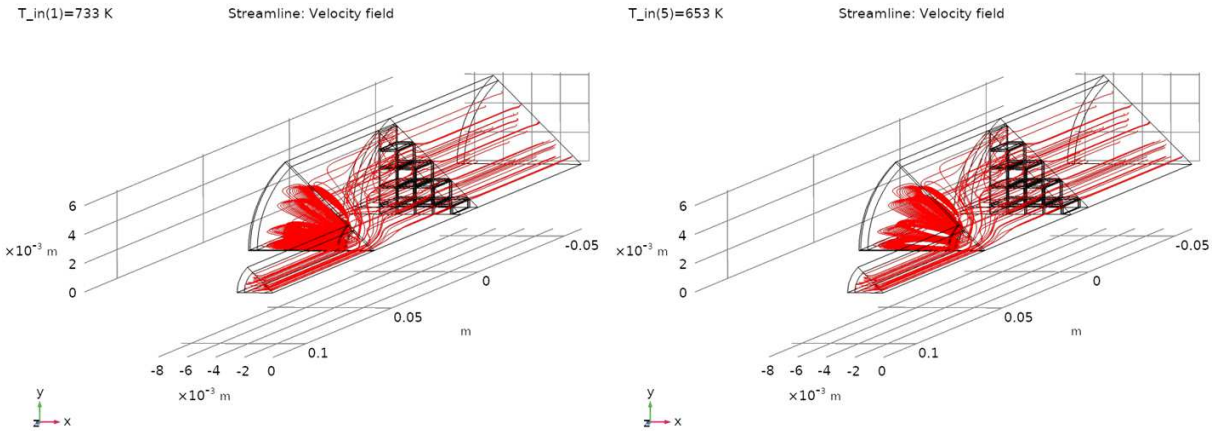

Figure 7. *The velocity magnitude (m/s) along the catalyst system. The catalyst used for 890 h at an inlet temperature of 733 K (left) and 653 K (right).*

Figure 7 shows how there is a giant swirl formed when the flow from the narrow inlet tube enters the larger quartz tube

before the monolith. The question arises whether this causes a maldistribution in temperature and inlet NH_3 content. The relative long distance from the inlet tube to the monolith works to make the velocity profile more even. After the catalyst, the flow is linear as it was in the inlet tube.

3.7. The Maldistribution of Ammonia Through the Catalyst

Figure 8 shows how ammonia is distributed over the system for the catalyst used for 890 h. The simulation gives 745.6 ppm at the reactor inlet. The correct inlet value is 745.6 ppm since this is the boundary condition. Because of heat effects the content of NH_3 at the catalyst inlet surface (Figure 8 top right) has decreased to between 728 and 697 ppm. At the outlet of the catalyst (Figure 8 bottom left) the content varies from 393 to 384 ppm with the lowest conversion in the center of the monolith where there is a higher velocity than other places.

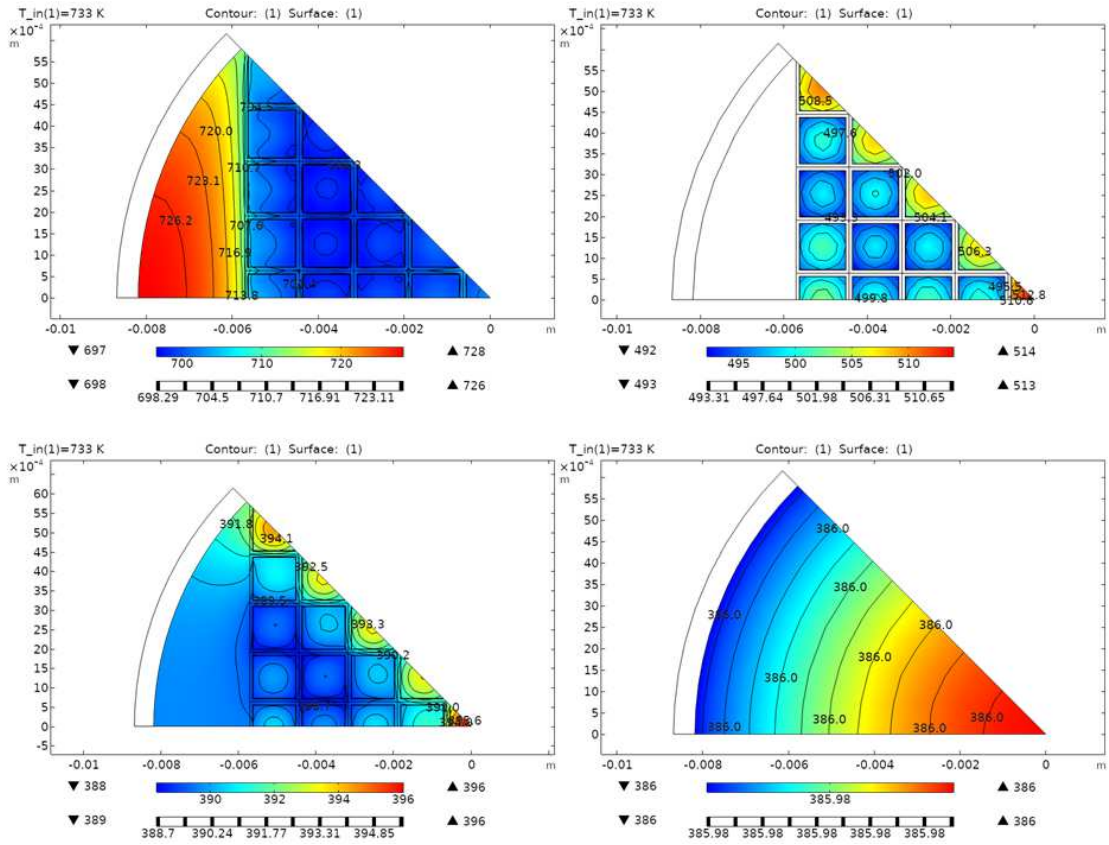

Figure 8. *The content of NH_3 (ppm) over the reactor cross-section at T=733 K for the catalyst used for 890 h and non-isothermal conditions. Top row to the left at the monolith inlet, to the right at 1 mm from the exit of the monolith (inside catalyst). Bottom row to the left at the monolith outlet and to the right at the reactor outlet. NH_3 inlet=745.6 ppm.*

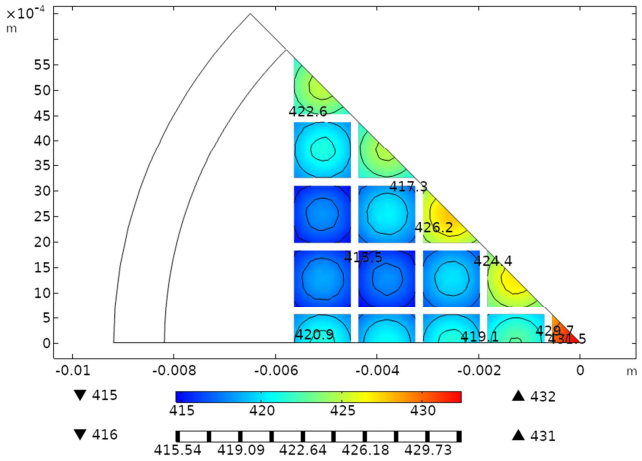

Figure 9. *The content of NH_3 (ppm) at an enlarged cross-section of the monolith 1 mm before its exit. The catalyst used for 2299 h. NH_3 inlet is 702 ppm.*

The concentration of ammonia at the reactor inlet is, by simulation, 745.6 pm over the whole cross section. 5 mm from the catalyst inlet the concentration varies from 492 to 514 ppm with conversions of 34.0 to 31.1%, respectively (not shown here). At 1 mm from the monolith exit, (Figure 8 top right) the value in the center is 408 ppm and the lowest 389 ppm somewhere inside the monolith. At the catalyst outlet the conversion varies from 48.5 to 47.3% (Figure 8 bottom left). Thus, the variation is not considerable. In the last part of the Figure 8 (bottom right), the reactor exit concentration is shown and it is 386 ppm, equal over the reactor cross section. Thus, here the conversion is 48.2% and it is even over the whole surface.

Figure 9 clearly shows the variation of the NH_3 content from 415 ppm in the three channels shown in blue to the left in the monolith to 432 ppm in the center channel (red). The higher content in the center is caused by the shorter residence time there (higher linear flow) and thus a lower conversion of

NH_3. The difference between the lowest and the highest concentration is but 4%.

3.8. The Maldistribution of NO

Figure 10 shows the simulated concentration of NO at the monolith exit for the catalyst used for 890 h and at 733 K. The distribution is uneven with the highest temperature in the center part of the catalyst monolith. The highest NO contents are observed in the pink areas in the Figure and are 13.7 ppm for the fresh catalyst, 24.1 ppm for the catalyst used for 890 h, and 38.2 ppm for the catalyst used for 2299 h. The lowest contents span from 13.4 via 23.6 to 37.1 ppm and are always seen in the center of the catalyst where the flow rate is largest. The total temperature increase is only 0.95 K at 733 K for the catalyst used for 2299 h. The low temperature maldistribution results in just a little smaller amount of the product NO in the center of the catalyst monolith as shown in Figure 10.

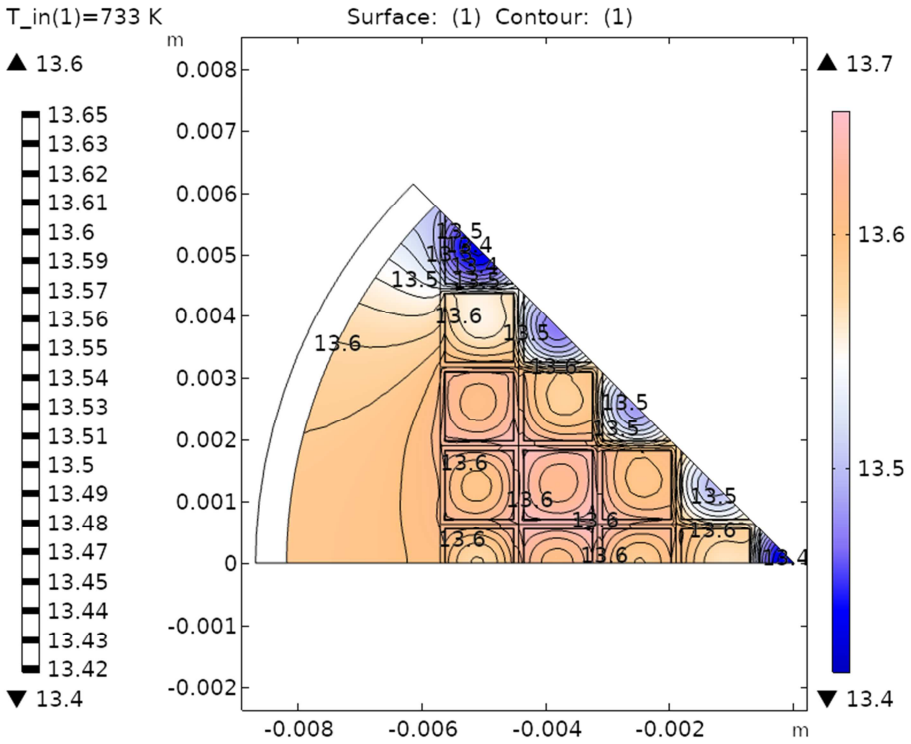

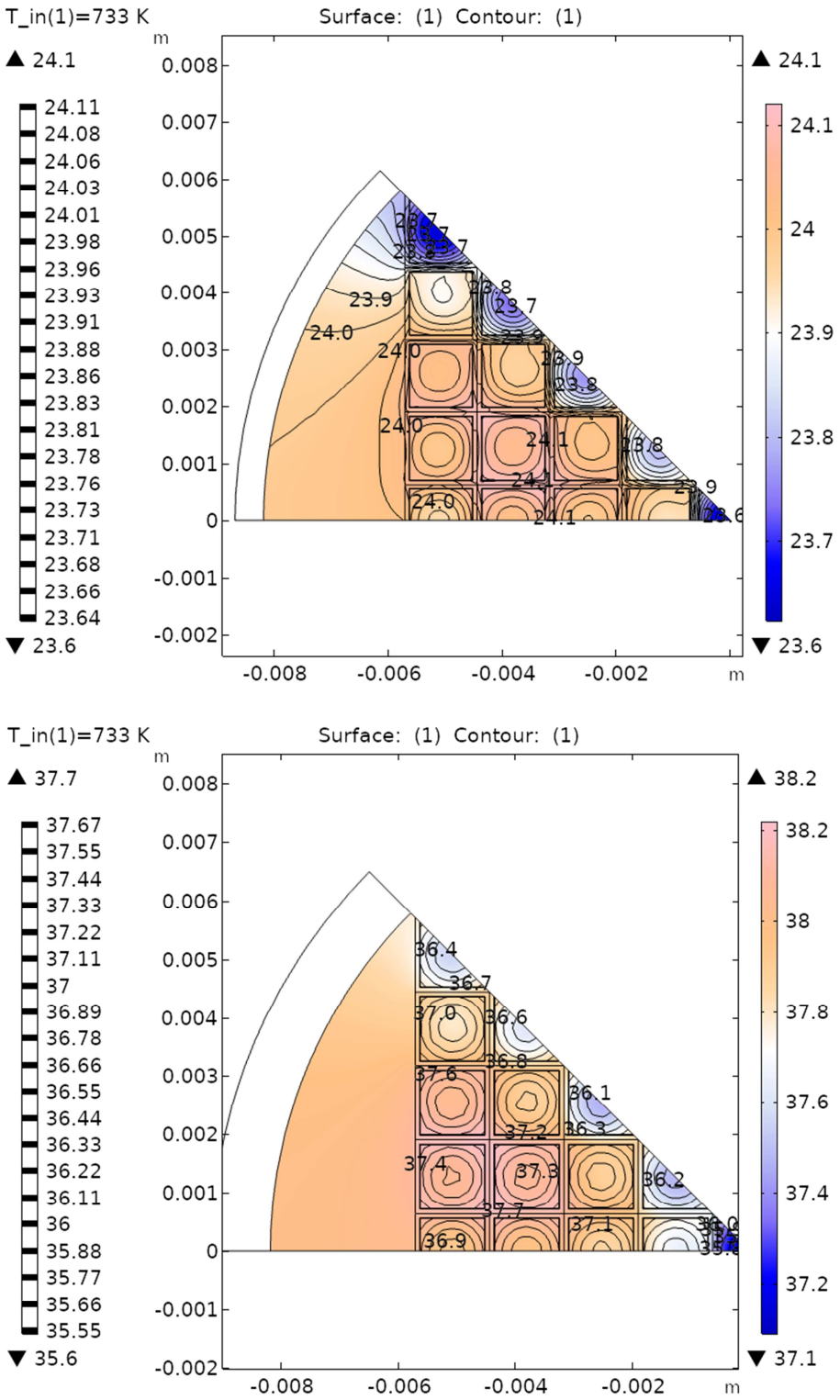

Figure 10. *The concentration of NO over the exit of the catalyst monolith at 733 K. Oxidation of about 700 ppm NH_3 with 2% O_2 over the three catalysts. Top, fresh catalyst, middle, the catalyst used for 890 h, bottom, the catalyst used for 2299 h.*

3.9. The Advantages of Using a Multichannel Model

The use of the multichannel model has several advantages, some of them have been shown in this example. It is of special importance to use a multichannel model if one has a special arrangement of the inflow as in the example presented here. The total temperature increase is meagre in the present example, but still effects are seen in variation of the conversion over the catalysts surface. It is the high flow in the inlet tube that causes a distinct higher flow also in the center part of the monolith. For more exothermic reactions and larger inlet flows the advantage of using the multichannel model are clear. The only disadvantage is that in this model it was

necessary to divide the monolith and reactor into 8 parts and only make simulation on one of them. This was necessary because of large memory demand and large computation time especially with an exceptionally fine mesh.

4. Conclusions

In the simulation of the of oxidation of ammonia with oxygen using a commercial Finite Element package it was shown that the three products nitrogen, nitrous oxide, and nitric oxide are formed at increasing temperatures. In the simulation, all three rates of oxidation of ammonia were supposed to be of first order in its concentration.

A multichannel model, including all the 9*9 channels, was used to study the effects of flow, concentration, and temperature maldistributions on the results. The effects were clear, albeit at low values. The maximal temperature increase was around 1.3 K at 733 K.

The kinetic parameters were shown to vary with the degree of deactivation. By simulation, the effect of deactivation on the kinetic parameters of the oxidation of ammonia was determined. A decrease of the activation energies with the degree of deactivation was observed for all reactions. Experimental rates were at maximum for the catalyst used for 890 h for the formation of N_2 and N_2O. The formation of NO increased continuously with the degree of poisoning.

There is quite a substantial reduction in BET surface area during the deactivation process. When the surface-specific rates were compared, the order of rates for the three catalysts remained the same even if absolute values decreased.

Acknowledgements

We wish to thank Mr. Martin Bruszt, who performed the reaction experiments. A Swedish diesel engine test company is acknowledged for supplying the fresh and deactivated catalyst samples as well as the testing unit. This simulation study did not receive any specific grants from funding agencies in the public, commercial, or not-for-profit sectors.

References

[1] A. Konstandopoulos, D. Zarvalis, L. Chasapidis, L. Deloglou, N. Vlachos, A. Kotbra, and G. Anderson, Investigation of SCR Catalysts for Marine Diesel Applications, SAE International Journal of Engines, Vol. 10 (4), pp. 1653-1666, 2017.

[2] C. U. I. Odenbrand, Penetration of Poisons Along the Monolith Length of a V_2O_5/TiO_2 Diesel SCR Catalyst and Its Effect on Activity, Catalysis Letters, Vol. 149 (12), pp. 3476-3490, 2019.

[3] C. U. I. Odenbrand, The kinetics of the oxidation of ammonia on a V_2O_5/TiO_2 catalyst deactivated in an engine rig. Part I. Determination of kinetic parameters by simulation, Environmental Research & Technology, Vol. 2 (4), pp. 211-221, 2019.

[4] U. S. Ozkan, Y. Cai, M. W. Kuthekar, and L. Zhang, Role of Ammonia Oxidation in Selective Catalytic Reduction of Nitric Oxide over Vanadia Catalysts, Journal of Catalysis, Vol. 142, pp. 182-197, 1993.

[5] U. S. Ozkan, Y. Cai, and M. W. Kuthekar, Investigation of the Mechanism of Ammonia Oxidation and Oxygen Exchange over Vanadia Catalysts Using N-15 and O-18 Tracer Studies, Journal of Catalysis, Vol. 149, pp. 375-389, 1994.

[6] B. L. Du y, H. E. Curry-Hyde, N. W. Cant, and P. F. Nelson, Isotopic Labelling Studies of the Effects of Temperature, Water and Vanadia Loading on the Selective Catalytic Reduction of NO with NH_3 over Vanadia-Titania Catalysts, Journal of Physical Chemistry, Vol. 98, pp. 7153-7161, 1994.

[7] A. M. Efstathiou, and K. Fliatoura, Selective catalytic reduction of nitric oxide with ammonia over V_2O_5/TiO_2 catalyst; A steady-state and transient kinetic study, Applied Catalysis B: Environmental., Vol. 6, pp. 35-59, 1995.

[8] S. Djerad, M. Crocoll, S. Kureti, L. Tifouti, and W. Weisweler, Effect of oxygen concentration on the NO_x reduction with ammonia over V_2O_5-WO_3/TiO_2 catalyst, Catalysis Today, Vol. 113, pp. 208-214, 2006.

[9] N. Usberti, M. Jablonska, M. Di Blasi, P. Forzatti, P. Lietti, Design of a "high-efficiency" NH_3-SCR reactor for stationary applications. A kinetic study of NH_3 oxidation and NH_3-SCR over V-based catalysts, Appl. Catal. B: Environ. Vol. 179, pp. 185-195, 2015.

[10] H. J. Chae, T. C. Cho, H. Choi, I.-S. Nam, H. S. Yang, S. L. Song, Direct Use of Kinetic Parameters for Modeling and Simulation of a Selective Catalytic Reduction Process, Ind. Eng. Chem. Res., Vol. 39, pp. 1159-1170.

[11] I. Nova, L. dall' Acqua, L. Lietti, E. Giamello, P. Forzatti, Study of thermal deactivation of a de-NO_x commercial catalyst, Appl. Catal. B: Environ. Vol. 35 (1), pp. 31-42, 2001.

[12] C.-T. Chen, W.-L. Tan, Mathematical modeling, optimal design and control of an SCR reactor for NO_x removal, J. of the Taiwan Institute of Chemical Engineers, Vol. 43, pp. 409-419, 2012.

[13] B. K. Yun, M. Y. Kim, Modeling the selective catalytic reduction of NO_x by ammonia over a Vanadia-based catalyst from heavy duty diesel exhaust gases, Appl. Thermal Engineering, Vol. 50, pp. 152-158. 2013.

[14] J. Om, P. Ji, W. Wu, 3D Numerical Simulation of Gas Flow and Selective Catalytic Reduction (SCR) of NO in the Honeycomb Reactor, Asia-Pacific Energy Equipment Engineering Research Conference (AP3ER 2015) pp. 56-65, 2015. Atlantis Press.

[15] F. Millo, M. Rafigh, D. Fino, P. Micelli, Application of a global kinetic model on an SCR coated on Filter (SCR-F) catalyst for automotive applications, Fuel Vol. 198, pp. 183-192, 2017.

[16] A. Åberg, A. Widd, J. Abildskov, J. Kjöbsted Huusom, Parameter estimation and analysis of an automotive heavy-duty SCR catalyst model, Chem. Eng. Sci., Vol. 161, pp. 167-177, 2017.

[17] Shin SB, Skau KI, Menon M, Maroor S, A modelling approach to kinetic study and novel monolith channel design for selective catalytic reduction (SCR) applications, Chem. Eng. Res. Des., Vol. 142, pp. 412-428, 2019.

[18] C. U. I. Odenbrand, High Temperature and High Concentration SCR of NO with NH_3 for the Oxyfuel Combustion Process:

Fitting of Kinetics to Data from a Laboratory Reactor Experiment, Topics in Catalysis, Vol. 60, pp, 1317-1332, 2017.

[19] C. U. I. Odenbrand, $CaSO_4$ deactivated V_2O_5- WO_3/TiO_2 SCR catalyst for a diesel power plant. Characterisation and simulation of the kinetics of the SCR reactions, Applied Catalysis B: Environmental, Vol. 234, pp. 365-377, 2018.

[20] J. G. M. Brandin, and C. U. I. Odenbrand, Poisoning of SCR Catalysts used in Municipal Waste Incineration Applications, Topics in Catalysis, Vol. 60, pp. 1306-1316, 2017.

[21] J. G. M. Brandin, and C. U. I. Odenbrand, Deactivation and Characterisation of SCR Catalysts Used in Municipal Waste Incineration Applications, Catalysis Letters, Vol. 148 (1), pp. 312-327, 2018.

[22] S. Salehi, M. A. Moghaddam, and N. Sahebjamee, Modeling Transport Phenomena in Selective Catalytic Reductant Catalytic Converter with NH_3 as reductant for NO Degradation, International Journal of Engineering, Vol. 29 (9), pp. 1183-1190, 2016.

[23] G. Schaub, D. Unruh, J. Wang, and T. Turek, Kinetic analysis of selective catalytic NO_x reduction (SCR) in a catalytic filter, Chemical Engineering and Processing, Vol. 42, pp. 365-371, 2003.

[24] J. Due-Hansen, A. L. Kustov, C. Hviid Christensen, and R. Fehrmann, Impact of support and potassium-poisoning on the V_2O_5-WO_3/ZrO_2 catalyst performance in the ammonia oxidation, Catalysis Communications, Vol. 10, pp. 803-806, 2009.